Journal of Bioanalysis & Biomedicine

Trivedi et al., J Bioanal Biomed 2015, 7:5
DOI: 10.4172/1948-593X.1000137

Research Article Open Access

Biofield Treatment: An Effective Strategy for Modulating the Physical and Thermal Properties of O-Nitrophenol, M-Nitrophenol and P-Tertiary Butyl Phenol

Mahendra Kumar Trivedi[1], Rama Mohan Tallapragada[1], Alice Branton[1], Dahryn Trivedi[1], Gopal Nayak[1], Rakesh K Mishra[2] and Snehasis Jana[2]*

[1]*Trivedi Global Inc., 10624 S Eastern Avenue Suite A-969, Henderson, USA*
[2]*Trivedi Science Research Laboratory Pvt. Ltd., Hall-A, Chinar Mega Mall, Chinar Fortune City, Madhya Pradesh, India*

Abstract

Phenolic compounds are commonly used for diverse applications such as in pharmaceuticals, chemicals, rubber, dyes and pigments. The objective of present research was to study the impact of Mr. Trivedi's biofield treatment on physical and thermal properties of phenol derivatives such as o-nitrophenol (ONP), m-nitrophenol (MNP) and p-tertiary butyl phenol (TBP). The study was performed in two groups (control and treated). The control and treated compounds were characterized using X-ray diffraction (XRD), differential scanning calorimetry (DSC), thermogravimetric analysis (TGA), and surface area analysis. XRD analysis showed increase in crystallite size by 16.05% in treated ONP as compared to control. However, the treated MNP showed decrease in crystallite size by 16.17% as compared to control. The treated TBP showed increase in crystallite size by 5.20% as compared to control. DSC of treated MNP exhibited increase in melting temperature with respect to control, which may be correlated to higher thermal stability of treated sample. However, the treated TBP exhibited no significant change in melting temperature with respect to control. TGA analysis of treated ONP and TBP showed an increase in maximum thermal decomposition temperature (T_{max}) as compared to control. However, the treated MNP showed slight decrease in T_{max} in comparison with control sample. Surface area analysis of treated ONP showed decrease in surface area by 65.5%. However, surface area was increased by 40.7% in treated MNP as compared to control. These results suggest that biofield treatment has significant effect on physical and thermal properties of ONP, MNP and TBP.

Keywords: Biofield treatment; O-nitrophenol; M-nitrophenol; P-tertiary butyl phenol; X-ray diffraction; Thermal analysis; Surface area

Abbreviations: ONP: O-nitrophenol; MNP: M-nitrophenol; TBP: P-tertiary butyl phenol; XRD: X-ray Diffraction; DSC: Differential Scanning Calorimetry; TGA: Thermogravimetric Analysis; FT-IR: Fourier Transform Infrared Spectroscopy; DTA: Differential Thermal Analyzer; DTG: Derivative Thermogravimetry

Introduction

The nitro phenol compounds are the largest and widely known group of industrial chemicals in use today. These compounds are organic molecules that contain at least one $-NO_2$ group attached to the aromatic ring [1]. Nitrophenols are commonly used in pharmaceuticals, wood preservatives, rubber chemicals, dyes, pigments, explosives and industrial solvents [2]. O-nitrophenol (ONP) and m-nitrophenol are important compounds which have been used as a reagent for synthesis of organic compounds [2]. Moreover, few nitrophenols are used as promising material for nonlinear optical and optoelectronic applications [3,4]. In order to attain this goal, these compounds not only have the presence of their electron donor "–OH" and electron acceptor "$-NO_2$" substituents but also they can form strong hydrogen bonds with other compounds [5]. On the other hand, p-tertiary butyl phenol (TBP) is used for synthesis of TBP- formaldehyde resins due their excellent oil solubility, adhesive property and low cost. However, the excess production of these phenol derivatives poses considerable challenge and health problems. Due to low biodegradability, high solubility, weak ionization capacity, phenol and its derivatives are commonly detected in surface water [6]. Hence, novel methods should be designed to modify the physicochemical properties of phenol based compounds in order to reduce the toxicity related issues. Biofield treatment had been altered the physical, crystalline and thermal properties of various metals powders [7-10].

Researchers have shown that human body functions as a macroscopic quantum system [11-14]. Feyman (1949) proposed scientific basis of quantum biology using quantum electrodynamics and chromodynamics [15]. In other words, each quantum system consists of quantum-domains which have some oscillators within that generate the potential field. Additionally, researchers have demonstrated that human physiology shows a high degree of order and stability due to their coherent dynamic states [16,17]. Thus, the human body emits the electromagnetic waves in form of bio-photons, which surrounds the body and it is commonly known as biofield. Therefore, the biofield consists of electromagnetic field, being generated by moving electrically charged particles (ions, cell, molecule etc.) inside the human body.

Furthermore, a human has ability to harness the energy from environment/universe and can transmit into any object (living or non-living) around the Globe. The object(s) always receive the energy and respond into useful way that is called biofield energy. Mr. Mahendra K.

***Corresponding author:** Snehasis Jana, Trivedi Science Research Laboratory Pvt. Ltd., Hall-A, Chinar Mega Mall, Chinar Fortune City, Hoshangabad Rd., Bhopal- 462026, Madhya Pradesh, India, Tel: +91-755-6660006; E-mail: publication@trivedisrl.com

Received July 14, 2015; **Accepted** September 08, 2015; **Published** September 11, 2015

Citation: Trivedi MK, Tallapragada RM, Branton A, Trivedi D, Nayak G, et al. (2015) Biofield Treatment: An Effective Strategy for Modulating the Physical and Thermal Properties of O-Nitrophenol, M-Nitrophenol and P-Tertiary Butyl Phenol. J Bioanal Biomed 7: 156-163. doi:10.4172/1948-593X.1000137

Trivedi is known to alter the characteristics of many things in several research fields such as, agriculture and biotechnology [18-21]. Biofield treatment has shown excellent results in improving the antimicrobial susceptibility pattern, and alteration of biochemical reactions, as well as induced alterations in characteristics of pathogenic microbes [22-24]. Exposure to biofield treatment caused an increase in medicinal property, growth, and anatomical characteristics of ashwagandha [25].

By conceiving the above research outcome of biofield treatment, an attempt was made here to study the influence of biofield on physical and thermal properties of phenol derivatives (ONP, MNP, and TBP).

Materials and Methods

ONP and MNP were procured from Loba Chemie Pvt., Ltd., India. TBP was procured from Sisco Research Laboratories (SRL), Pvt., Ltd., India.

Biofield treatment

ONP, MNP and TBP were divided into two parts; one was kept as a control sample, while the other was subjected to Mr. Trivedi's biofield treatment and coded as treated sample. The treatment group was in sealed pack and handed over to Mr. Trivedi for biofield treatment under laboratory condition. Mr. Trivedi provided the treatment through his energy transmission process to the treated group without touching the sample. After biofield treatment the control and treated group was subjected to physicochemical characterization under standard laboratory conditions.

Characterization

X-ray diffraction (XRD) study: XRD analysis was carried out on Phillips, Holland PW 1710 X-ray diffractometer system, which had a copper anode with nickel filter. The radiation of wavelength used by the XRD system was 1.54056 Å. The data obtained from this XRD were in the form of a chart of 2θ vs. intensity and a detailed table containing peak intensity counts, d value (Å), peak width (θ°), relative intensity (%) etc. The crystallite size (G) was calculated by using formula:

$$G = k\lambda/(b\cos\theta)$$

Where, λ is the wavelength and k is the equipment constant (0.94).

$$\text{Percent change in crystallite size} = [(G_t - G_c)/G_c] \times 100$$

Where, G_c and G_t are crystallite size of control and treated powder samples respectively.

Differential scanning calorimetry (DSC) study: The control and treated samples (ONP, MNP, and TBP) were analyzed by using a Pyris-6 Perkin Elmer DSC on a heating rate of 10°C/min under air atmosphere and air was flushed at a flow rate of 5 mL/min. A predetermined amount of sample was weighed and kept in the DSC aluminum pan. A covered aluminum pan was used as a DSC reference pan.

Thermogravimetric analysis-differential thermal analysis (TGA-DTA): Thermal stability of control and treated samples (ONP, MNP, and TBP) were analyzed by using Mettler Toledo simultaneous TGA and Differential thermal analyzer (DTA). The samples were heated from room temperature to 400°C with a heating rate of 5°C/min under air atmosphere.

Surface area analysis: The surface area of control and treated ONP and MNP were characterized by surface area analyzer, SMART SORB 90 BET using ASTM D 5604 method which had a detection range of 0.2-1000 m^2/g. Percent change in surface area was calculated using following equation:

$$\%\ \text{change in surface area} = [S_{Treated} - S_{Control}]/S_{Control} \times 100$$

Where, $S_{Control}$ and $S_{Treated}$ are the surface area of control and treated samples respectively.

Results and Discussion

X-ray diffraction

XRD was conducted to study the crystalline nature of ONP, MNP and TBP after biofield treatment. The XRD diffractogram of control and treated ONP are presented in Figure 1. The XRD graphs of control ONP showed the presence of intense crystalline peaks at 2θ equals to 12.25°, 15.37°, 17.99°, 18.66°, 23.2°, 24.66°, 26.97°, 27.34°, 27.65° and 29.12°. Whereas the treated sample showed peaks at 2θ equals to 12.24°, 12.45°, 15.27°, 15.51°, 18.70°, 23.33°, 27.00°, 27.36°, 19.13°, and 30.05°. The comparative evaluation showed that after biofield treatment the intensity of XRD peaks was decreased as compared to control. This may be correlated with the reduction in crystallinity of the treated ONP. It is hypothesized that biofield treatment may disturb the symmetrical order of the crystals that reduced the crystallinity. Crystallite size was calculated using Scherrer formula (crystallite size = kλ/b cos θ), and results are presented in Table 1 and Figure 2. The crystallite size is one of the crystallographic factors associated with the formation of dislocations and point defects in the crystalline structure,

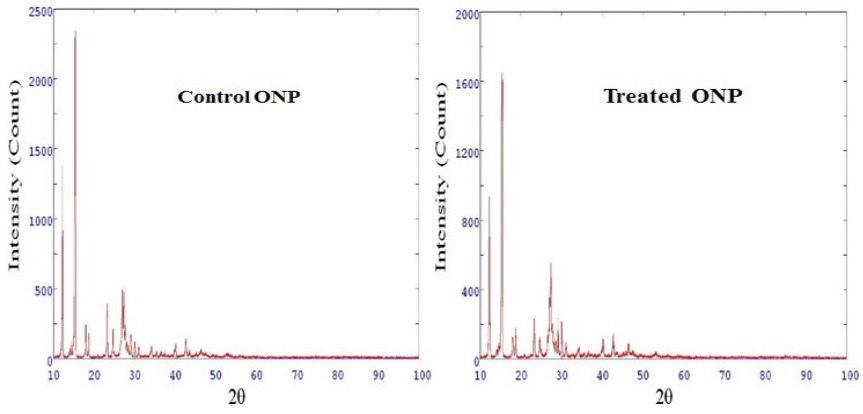

Figure 1: XRD diffractogram of o-nitrophenol (ONP).

Sample	Control (nm)	Treated (nm)
o-nitrophenol	80.96	93.96
m-nitrophenol	104.67	87.74
p-tert butyl phenol	79.73	83.88

Table 1: Crystallite size (nm) of o-nitrophenol, m-nitrophenol and p-tertiary butyl phenol.

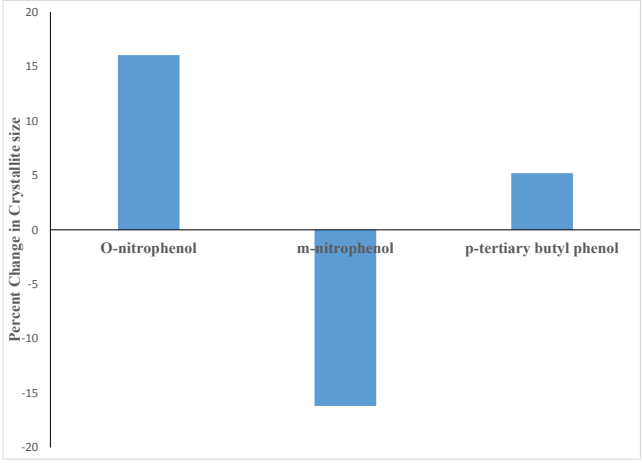

Figure 2: Percentage change in crystallite size of ONP, MNP and TBP.

which directly influences the material properties [26]. The control ONP showed crystallite size 80.96 nm, however, it was increased to 93.96 nm in treated ONP. The increase in crystallite size was 16.05% in the treated ONP as compared to control sample. In a previous work, it was shown that increase in temperature causes a considerable impact on crystallite size. It was also reported that increase in temperature reduced the thermodynamically driven force that caused a decrease in nuclear densities and thus increased in crystallite size [27,28]. Gaber *et al.* showed that elevation in processing temperature caused the decrease in dislocation density and increase in number of unit cell that ultimately increased the crystal growth [29]. Hence, it is assumed that biofield treatment may provide energy to ONP that leads to depression in nuclear density and elevation in crystallite size.

XRD diffractogram of control and treated MNP are shown in Figure 3. The control sample showed crystalline peaks at 2θ equals to 14.99°, 15.21°, 18.69°, 20.42°, 27.00°, 27.44°, 30.43°, 30.71°, 36.43°, 36.73°, and 40.97°. Whereas the treated MNP showed an increase in the intensity of the XRD peaks. The figure showed (Figure 3) peaks at 2θ equals to 12.43°, 12.59°, 15.21°, 18.67°, 20.32°, 20.46°, 21.75°, 27.04°, 27.40°, 30.70° and 36.68°. The comparative analysis showed that intensity of few XRD peaks were significantly increased with respect to control. It is presumed that biofield treatment may cause the crystal to come together and form regular lattice arrangement leading to increase in crystallinity. The crystallite size of control MNP was 104.67 nm, and it was decreased in treated MNP (87.74 nm). The decrease in crystallite size was 16.17% in treated MNP as compared to control sample. It is hypothesized that presence of the internal strains might be a reason for fracturing the grains into sub grains which leads to decrease in crystallite size of treated MNP.

XRD of control and treated TBP are presented in Figure 4. The XRD diffractogram displayed intense crystalline nature with peak at 2θ equals to 14.90°, 15.44°, 15.58°, 16.02°, 16.21°, 16.39°, 16.84°, 17.29°, 18.40°, 18.76°, 20.75°, 21.21°, 22.67°, and 25.76°. Whereas the treated

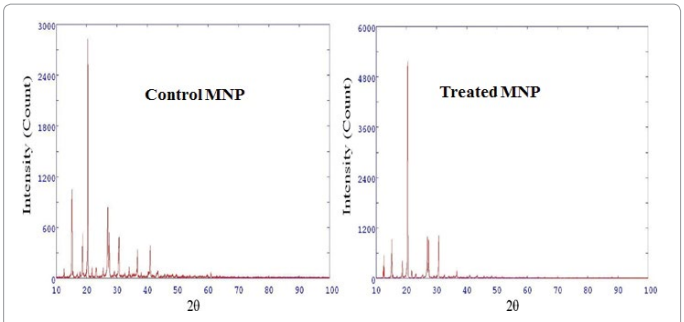

Figure 3: XRD diffractogram of m-nitrophenol (MNP).

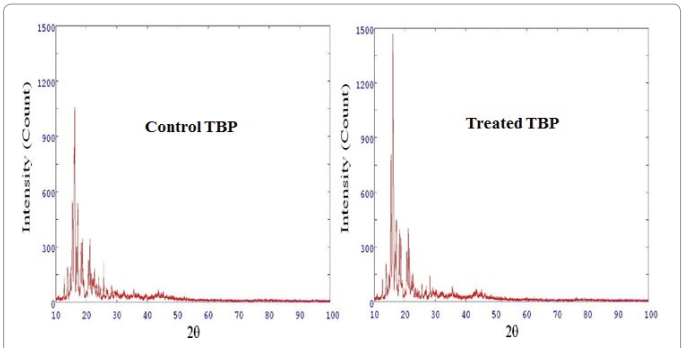

Figure 4: XRD diffractogram of p-tertiary butyl phenol (TBP).

compound showed (Figure 4) XRD peaks at 2θ equals to 13.88°, 15.45°, 16.05°, 16.34°, 16.75°, 17.11°, 17.28°, 18.35°, 18.72°, 20.62°, 20.75°, 21.17° and 21.52°. It was observed that intensity of few XRD peaks were increased due to alteration in crystalline nature of the treated sample. Crystallite size of control TBP was 79.73 nm, whereas the treated TBP showed 83.88 nm. The increase in crystallite size of treated TBP was 5.20% with respect to control. Biofield treatment on TBP probably caused depression in dislocation density hence increase in crystallite size [27]. Carballo *et al.*, reported that rate of reaction can be significantly improved by increase in crystallite size [30]. Hence, treated ONP and TBP due to high crystallite size may improve the reaction rate and percentage yield during synthesis of organic compounds.

DSC studies

DSC was used to investigate the melting nature and latent heat of fusion of the compounds (ONP, MNP and TBP). The melting temperature and latent heat of fusion of the compounds are shown in Table 2. The treated and control ONP did not show melting temperature peak in the DSC result. The control MNP showed (Table 2) endothermic peak at 98.07°C due to melting temperature of the sample [31]. Whereas the treated MNP showed an increase in melting temperature and it was observed at 99.50°C. This increase in melting temperature may be related to the higher thermal stability of the treated MNP. The control TBP showed an endothermic peak at 101.16°C; mainly due to melting of the control sample. However, the treated TBP showed melting endothermic peak at 101.33°C. The result showed no significant change in melting temperature of treated TBP in comparison with control.

The treated MNP showed an increase in ΔH value by 6.21% with respect to control. Similarly, the treated TBP compound showed the marked increase in ΔH by 14.48% as compared to control sample. It was reported that a material consists of strong intermolecular forces that

hold them tightly on their positions. The energy needed to overcome the intermolecular force is known as latent heat of fusion. This latent heat of fusion is stored as potential energy in the atoms during its phase transition from solid to liquid [32,33]. It is assumed that biofield treatment may altered the internal potential energy in treated MNP and TBP that leads to increase in ΔH as compared to control.

TGA studies

TGA was used to evaluate the thermal stability of the organic compounds. TGA thermogram of the control and treated ONP are shown in Figures 5 and 6 respectively. Thermogram of control sample showed (Figure 5) single step thermal degradation pattern. The thermal degradation commenced at around 118°C and terminated at around 158°C. During this step, the sample lost 62.54% of its weight. TGA thermogram of treated ONP showed (Figure 6) that thermal degradation started at around 125°C and stopped at around 170°C. During this thermal process, the sample lost 66.94% of its weight. DTA thermogram of control sample showed an endothermic peak at 146.03°C; however, the treated sample showed the increase in endothermic peak (152.71°C). DTG thermogram of control sample showed maximum thermal decomposition temperature (T_{max}) at 136.40°C. However, the treated sample showed an increase in T_{max} value at 144.91°C; that may be correlated to the higher thermal stability of the treated sample.

TGA thermogram of control and treated MNP are depicted in Figure 7 and 8, respectively. TGA thermogram of MNP showed onset temperature at around 193°C and it stopped at around 233°C (end set). During this step the control sample lost 60.30% of its weight (Figure 7). However, the treated sample started to degrade at around 188°C and this process terminated at around 242°C. The treated sample showed 52.39% weight loss. The DTA thermogram of control MNP showed two endothermic peaks. The first peak at 97.21°C was attributed to melting of the sample and second endothermic peak was due to thermal decomposition of control (217.94°C). DTA thermogram of treated MNP showed (Figure 8) no significant change in melting temperature but it showed an increase in decomposition temperature (220.10°C) as compared to control. However, the DTG thermogram of control showed the T_{max} at 209.81°C; whereas the treated sample showed the T_{max} at 208.21°C. This showed no significant alteration in thermal stability of treated MNP as compared to control.

TGA thermogram of control and treated TBP are shown in Figures 9 and 10 respectively. The control TBP showed one-step thermal degradation pattern. The thermal degradation commenced at around 137°C and terminated at around 198°C. The control sample lost 58.08% of its compound weight (Figure 9). The TGA thermogram of treated TBP also showed one-step thermal degradation pattern. The thermal degradation commenced at around 142°C (onset) and terminated at around 204°C (end set). DTA thermogram of the control TBP showed two endothermic peaks. The first peak at 102.55°C was due to melting and second peak at 175.54°C was due to decomposition of the sample. However, DTA thermogram of treated TBP showed (Figure 10) first endothermic peak at 103.54°C and the second peak was observed at

Sample	Melting Temperature (°C)		(ΔH J/g)		% Change in ΔH
	Control	Treated	Control	Treated	
o-nitrophenol	NO	NO	NO	NO	NO
m-nitrophenol	98.07	99.50	-141.45	-150.24	6.21
p-tert butyl phenol	101.16	101.33	-143.00	-164.18	14.81
NO-not observed					

Table 2: DSC data (Melting temperature and change in ΔH) of o-nitrophenol, m-nitrophenol and p-tert butyl phenol.

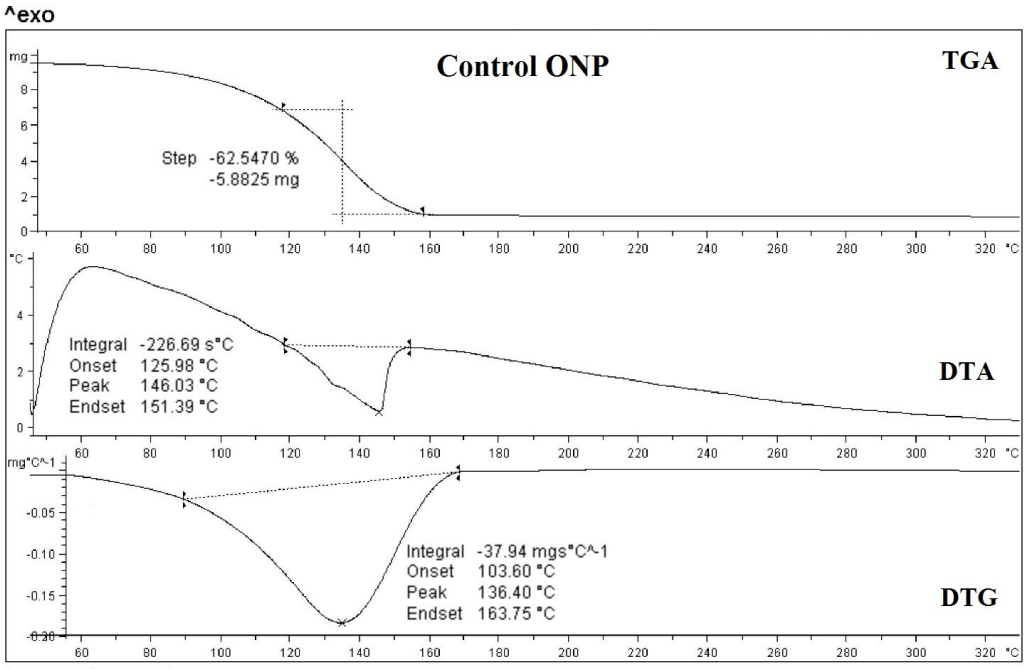

Figure 5: TGA thermogram of control o-nitrophenol (ONP).

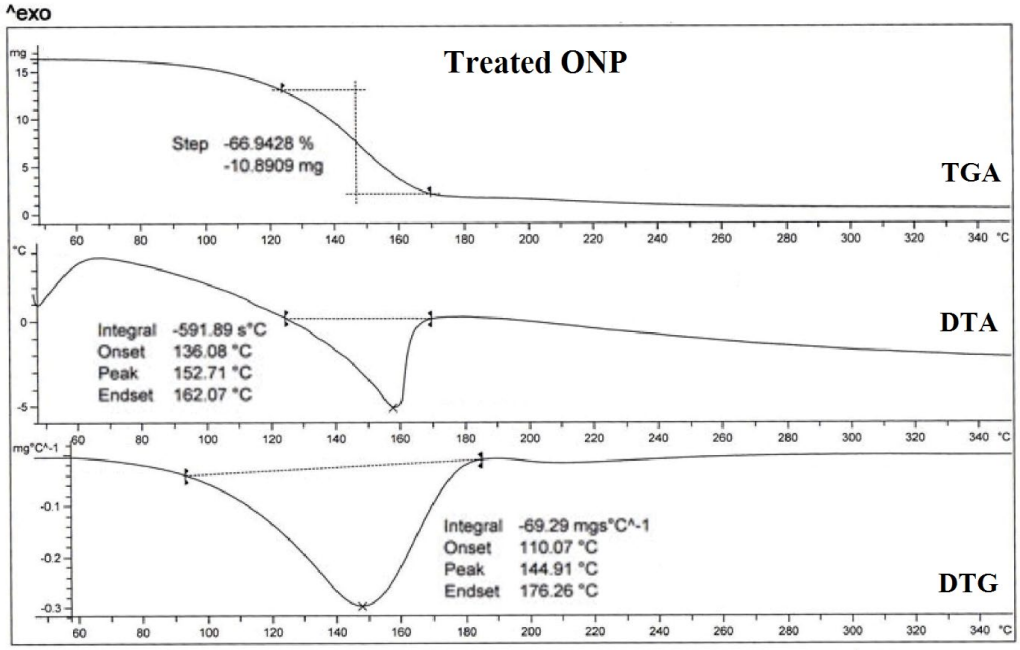

Figure 6: TGA thermogram of treated o-nitrophenol (ONP).

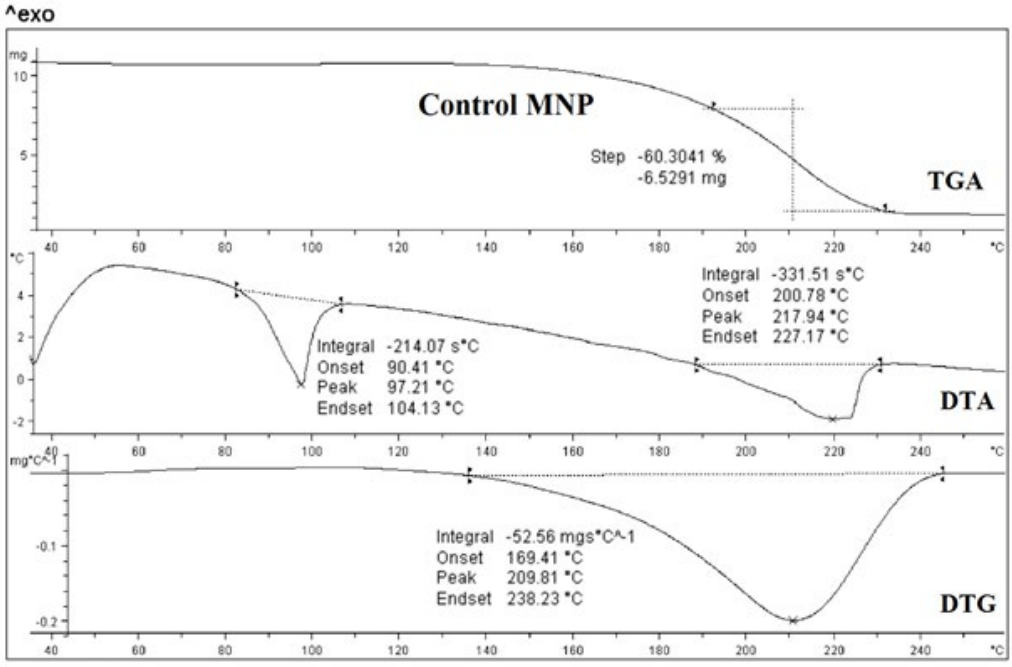

Figure 7: TGA thermogram of control m-nitrophenol (MNP).

180.13°C. The former peak was mainly due to melting temperature and latter peak was due to thermal decomposition of the compound. The DTG thermogram of control TBP showed T_{max} at 162.13°C. Additionally, the T_{max} of treated TBP (167.40°C) was increased as compared to T_{max} of the control sample. Szabo *et al.* showed that gamma radiation influenced the thermal stability of poly (3-hexadecylthiophene). They reported that increase in gamma radiation dose causes elevation in thermal stability due to crosslinking and conformational changes in the side alkyl groups [34]. Hence, it is assumed that biofield treatment may cause crosslinking in ONP and TBP molecules that lead to increase in thermal stability.

Surface area analysis

Surface area of the control and treated compounds were analyzed by using BET method and the results are presented in Table 3. The surface area of control ONP was 0.429 m^2/g; however, it was decreased in treated ONP (0.147 m^2/g). The decrease in surface area was 65.5%

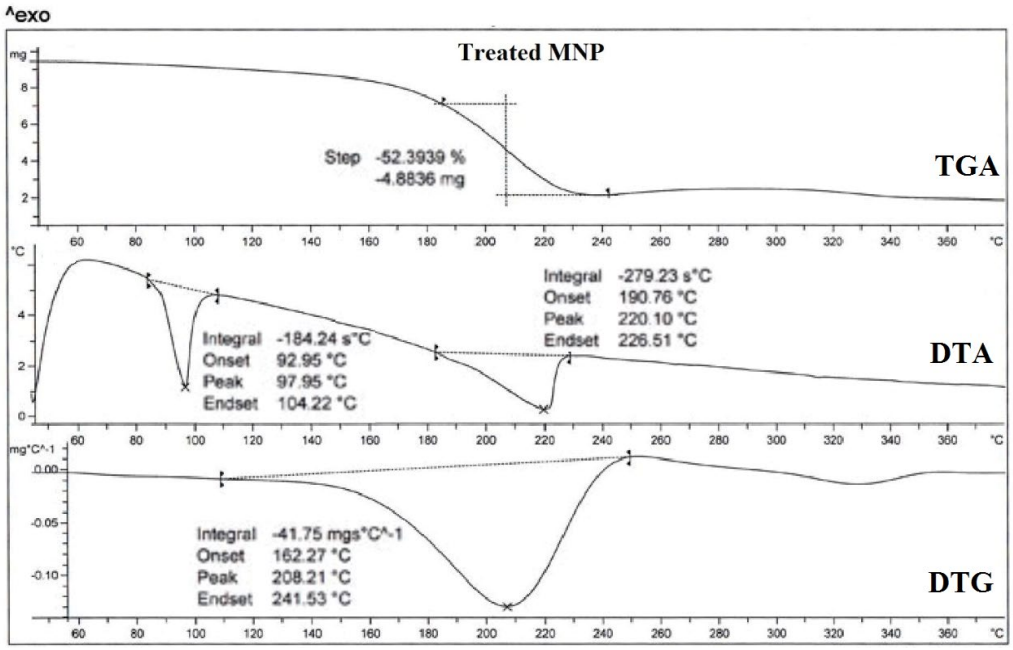

Figure 8: TGA thermogram of treated m-nitrophenol (MNP).

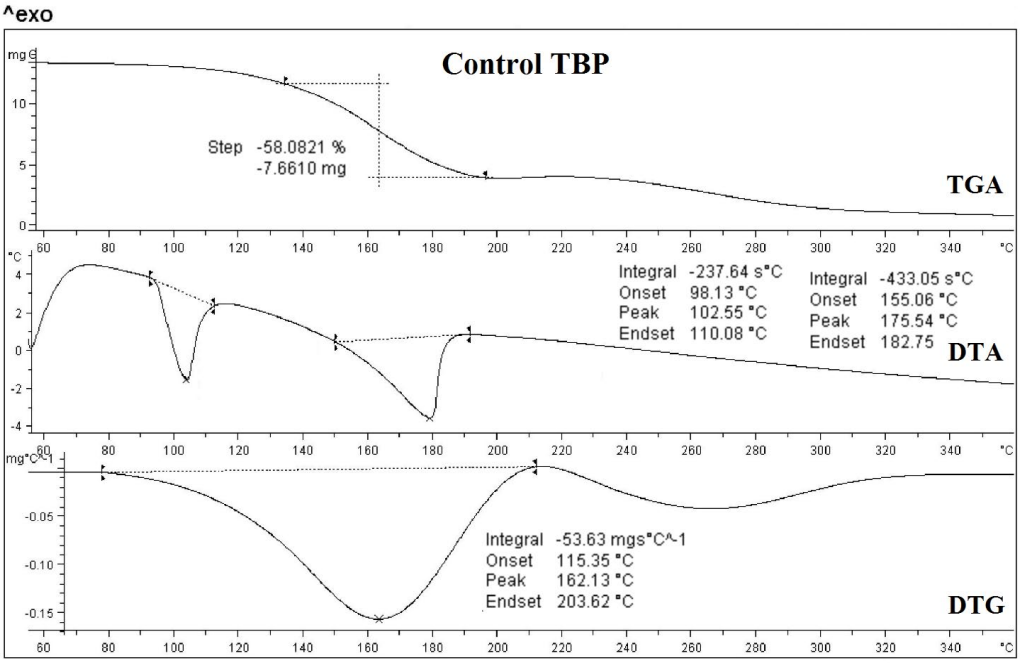

Figure 9: TGA thermogram of control p-tertiary butyl phenol (TBP).

as compared to control sample. This significant decrease in surface area may be due to increase in particle size of the treated ONP. It was reported that decrease in particle size increases the surface area and vice versa [35,36].

The surface area of control and treated MNP are reported in Table 3. The control MNP showed surface area of 0.214 m^2/g; however, it was increased in treated MNP (0.301 m^2/g). The increase in surface area was 40.7% in treated MNP as compared to control. The increase in surface area may be due to decrease in particle size of the treated MNP after biofield treatment. A similar increase in surface area was observed by Bergamaschi *et al.,* during their studies on lignin [37].

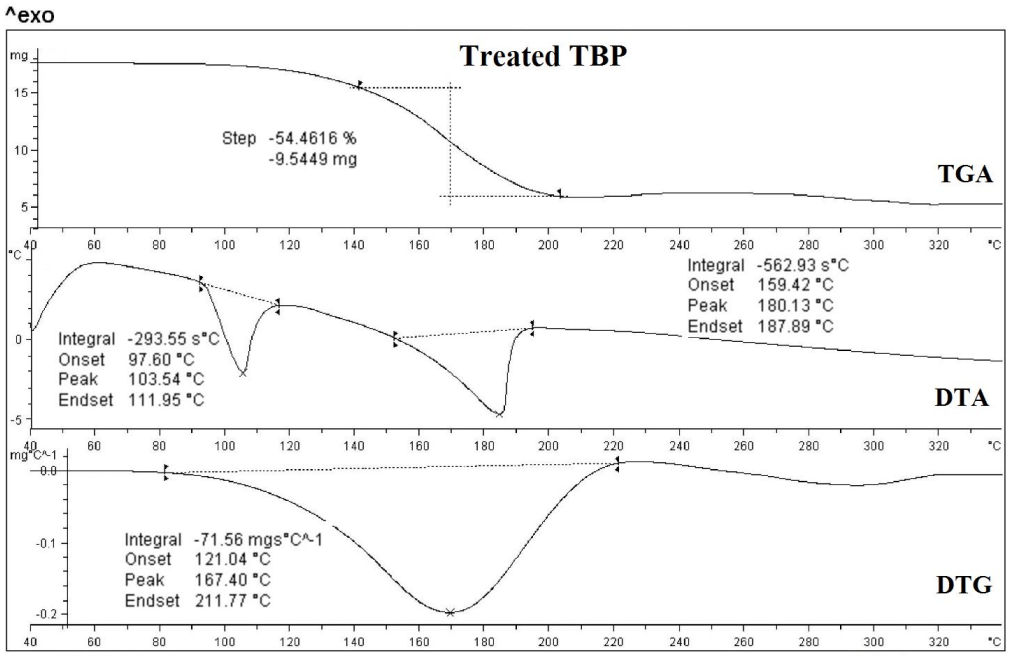

Figure 10: TGA thermogram of treated p-tertiary butyl phenol (TBP).

Sample	Control (m^2/g)	Treated (m^2/g)	% Change in surface area
o-nitrophenol	0.429	0.1479	-65.5
m-nitrophenol	0.214	0.301	40.7
p-Tert butyl phenol	ND	ND	ND
ND-not done			

Table 3: Surface area analysis of o-nitrophenol, m-nitrophenol and p-tert butyl phenol.

Conclusion

This research work evaluated the influence of biofield treatment on physical and thermal properties of phenolic compounds such as ONP, MNP and TBP. XRD study revealed increase in crystallite size of the treated ONP and TBP as compared to control. However, the treated MNP showed a decrease in crystallite size with respect to control. The treated MNP showed increase in melting as compared to control sample. However, TBP did not show a significant change in melting temperature. TGA analysis showed the enhanced thermal stability of the treated ONP and TBP as compared to control. However, no significant change in thermal stability of treated MNP was observed with respect to control. Overall, the results showed that biofield treatment has the significant impact on physical and thermal properties of the ONP, MNP and TBP.

Acknowledgement

The authors would like to thank all the laboratory staff of MGV Pharmacy College, Nashik for their assistance during the various instrument characterizations. The authors would also like to thank Trivedi Science, Trivedi Master Wellness and Trivedi Testimonials for their support during the work.

References

1. Ju KS, Parales RE (2010) Nitroaromatic compounds, from synthesis to biodegradation. Microbiol Mol Biol Rev 74: 250-272.
2. Liao Q, Sun J, Gao L (2008) The adsorption of resorcinol from water using multi-walled carbon nanotubes. Colloids Surf A 312: 160-165.
3. Wang LN, Wang XQ, Zhang GH, Liu XT, Sun ZH, et al. (2011) Single crystal growth, crystal structure and characterization of a novel crystal: L-arginine 4-nitrophenolate 4-nitrophenol dehydrate (LAPP). J Cryst Growth 327: 133-139.
4. Chen T, Sun Z, Li L, Wang S, Wang Y, et al. (2012) Growth and characterization of a nonlinear optical crystal-2,6-diaminopyridinium4-nitrophenolate4-nitrophenol (DAPNP). J Cryst Growth 338: 157-161.
5. Muthuraman M, Beucher MB, Masse R, Nicoud JF, Desiraju GR (1999) Sodium 4-nitrophenolate 4-nitrophenol dihydrate crystal: a new herringbone structure for quadratic nonlinear optics. J Mater Chem 9: 1471-1479.
6. Hamidouche S, Bouras O, Zermane F, Cheknane B, Houari M, et al. (2015) Simultaneous sorption of 4-nitrophenol and 2-nitrophenol on a hybrid geocomposite based on surfactant-modified pillared-clay and activated carbon. Chem Eng J 279: 964-972.
7. Trivedi MK, Patil S, Tallapragada RM (2013) Effect of biofield treatment on the physical and thermal characteristics of vanadium pentoxide powders. J Mater Sci Eng S11: 001.
8. Trivedi MK, Patil S, Tallapragada RM (2013) Effect of biofield treatment on the physical and thermal characteristics of silicon, tin and lead powders. J Mater Sci Eng 2: 125.
9. Trivedi MK, Patil S, Tallapragada RM (2014) Atomic, crystalline and powder characteristics of treated zirconia and silica powders. J Mater Sci Eng 3: 144.
10. Trivedi MK, Patil S, Tallapragada RMR (2015) Effect of biofield treatment on the physical and thermal characteristics of aluminium powders. Ind Eng Manag 4: 151.
11. Del Giudice E, Doglia S, Milani M (1989) Magnetic flux quantization and josephson behavior in living systems. Phys Scrip 40: 786-791.
12. Nobili R (1985) Schrödinger wave holography in brain cortex. See comment in PubMed Commons below Phys Rev A 32: 3618-3626.

13. Popp FA (1989) Electromagnetic Bio-Information. Munchen, Baltimore: Urban & Schwarzenberg.

14. Smith CW (1998) Is a living system a macroscopic quantum system? Frontier Perspect 7: 9-15.

15. Feynman RP (1949) Space-time approaches to quantum electrodynamics. Phys Rev 76: 769-782.

16. Popp FA, Chang JJ, Herzog A, Yan Z, Yan Y (2002) Evidence of non-classical (squeezed) light in biological systems. Phys Lett 293: 98-102.

17. Popp FA, Quao G, Ke-Hsuen L (1994) Biophoton emission: experimental background and theoretical approaches. Mod Phys Lett B 8: 21-22.

18. Shinde V, Sances F, Patil S, Spence A (2012) Impact of biofield treatment on growth and yield of lettuce and tomato. Aust J Basic Appl Sci 6: 100-105.

19. Sances F, Flora E, Patil S, Spence A, Shinde V (2013) Impact of biofield treatment on ginseng and organic blueberry yield. Agrivita J Agric Sci 35: 22-29.

20. Lenssen AW (2013) Biofield and fungicide seed treatment influences on soybean productivity, seed quality and weed community. Agricultural Journal 8: 138-143.

21. Patil SA, Nayak GB, Barve SS, Tembe RP, Khan RR (2012) Impact of biofield treatment on growth and anatomical characteristics of Pogostemon cablin (Benth.). Biotechnology 11: 154-162.

22. Trivedi MK, Patil S (2008) Impact of an external energy on Staphylococcus epidermis [ATCC –13518] in relation to antibiotic susceptibility and biochemical reactions – An experimental study. J Accord Integr Med 4: 230-235.

23. Trivedi MK, Patil S (2008) Impact of an external energy on Yersinia enterocolitica [ATCC –23715] in relation to antibiotic susceptibility and biochemical reactions: An experimental study. Internet J Alternative Med 6: 2.

24. Trivedi MK, Bhardwaj Y, Patil S, Shettigar H, Bulbule A (2009) Impact of an external energy on Enterococcus faecalis [ATCC – 51299] in relation to antibiotic susceptibility and biochemical reactions – An experimental study. J Accord Integr Med 5: 119-130.

25. Nayak G, Altekar N (2015) Effect of biofield treatment on plant growth and adaptation. J Environ Health Sci 1: 1-9.

26. Ohira T, Yamamoto O (2012) Correlation between antibacterial activity and crystallite size on ceramics. Chem Eng Sci 68: 355-361.

27. Rashidi AM, Amadeh A (2009) The effect of saccharin addition and bath temperature on the grain size of nanocrystalline nickel coatings. Surf Coat Technol 204: 353-358.

28. Gusain D, Srivastava V, Singh VK, Sharma YC (2014) Crystallite size and phase transition demeanor of ceramic steel. Mater Chem Phys 145: 320-326.

29. Gaber A, Abdel-Rahim MA, Abdel-Latief AY, Abdel-Salam MN (2014) Influence of calcination temperature on the structure and porosity of nanocrystalline SnO2 synthesized by a conventional precipitation method. Int J Electrochem Sci 9: 81-95.

30. Carballo LM, Wolf EE (1978) Crystallite size effects during the catalytic oxidation of propylene on Pt/?-Al2O3. J Catal 53: 366-373.

31. Musuc AM, Razus D, Oancea D (2002) Investigation of thermal stability of some nitroaromatic derivatives by DSC. Analele Universitatii Bucuresti: Chimie 147-152.

32. Moore J (2010) Chemistry: The molecular science (4th edition), Brooks Cole.

33. Trivedi MK, Tallapragada RM, Branton A, Trivedi A, Nayak G, et al. (2015) Biofield Treatment: A potential strategy for modification of physical and thermal properties of indole. J Environ Anal Chem 2: 152.

34. Szabo L, Cik G, Lensy J (1996) Thermal stability increase of doped poly (hexadecylthiophene) by ?-radiation. Synt Met 78: 149-153.

35. Mennucci B, Martinez JM (2005) How to model solvation of peptides? Insights from a quantum-mechanical and molecular dynamics study of N-methylacetamide. I. Geometries, infrared, and ultraviolet spectra in water. J Phys Chem B 109: 9818-9829.

36. Bendz D, Tüchsen PL, Christensen TH (2007) The dissolution kinetics of major elements in municipal solid waste incineration bottom ash particles. J Contam Hydrol 94: 178-194.

37. Bergamaschi BA, Tsamakis E, Keil RG, Eglinton TI, Montluçon DB, et al. (1997) The effect of grain size and surface area on organic matter, lignin and carbohydrate concentration, and molecular compositions in Peru Margin sediments. Geochim Cosmochim ac 61: 1247-1260.